Revue Internationale
de Géomatique

Tech Science Press

https://doi.org/10.32604/rig.2026.084921

ARTICLE

Urbanization-Driven Indirect Effects on Vegetation: Spatial Heterogeneity and Long- and Short-Run Dynamics in Nanjing

Xiankai Ji[1,2], **Manchun Li**[1,2,*] **and Nan Xia**[1,2,3]

[1]Department of Geographic Information Science, School of Geography and Ocean Science, Nanjing University, Nanjing, China
[2]Jiangsu Provincial Key Laboratory of Geographic Information Science and Technology, Nanjing University, Nanjing, China
[3]Collaborative Innovation Center for the South Sea Studies, Nanjing University, Nanjing, China

*Corresponding Author: Manchun Li. Email: limanchun@nju.edu.cn

Received: 01 May 2026; Accepted: 25 May 2026; Published: 11 June 2026

ABSTRACT: Against the backdrop of rapid global urbanization, revealing the indirect ecological effects triggered by urban environmental restructuring and human management interventions carries early-warning significance for preventing cliff-like vegetation degradation driven by unchecked urban expansion. Existing studies predominantly rely on linear assumptions and neglect the temporal lags inherent in ecological responses, making it difficult to capture the long-run and short-run dynamics as well as potential nonlinear thresholds of indirect impacts. Using Nanjing as the study region, this research constructs a spatiotemporal panel dataset at 1 km × 1 km resolution based on multi-source remote sensing data from 2001–2018. Building upon the quantification of urbanization's indirect effects on vegetation, we introduce a panel CS-ARDL model (Cross-Sectionally Augmented Autoregressive Distributed Lag model) to decompose short-run dynamic shocks from long-run equilibrium effects. Results reveal that urban construction land continues to expand along the Yangtze River axis, forming a "core–corridor–cluster" spatial pattern. Concurrently, vegetation indirect effects display pronounced north–south spatial differentiation: the Yangtze River's north bank (exemplified by Luhe District) exhibits clustering of negative indirect effects, whereas the core urban area south of the Yangtze generally exhibits positive responses, accompanied by a synchronized evolution from "negative–weakly negative–shifting toward positive" across the study period. ARDL (Augmented Autoregressive Distributed Lag model) results further demonstrate that the short-run scale exhibits stronger spatial heterogeneity and volatility. At the long-run scale, urbanization's indirect effects on vegetation are predominantly positive, displaying a declining gradient of "core urban areas > suburban areas > rural areas"; however, significant clusters of negative long-run effects persist in both core urban zones and far-suburban expansion edges.

KEYWORDS: Urbanization; vegetation index; indirect effects; CS-ARDL model

1 Introduction

Global urbanization continues to advance. The latest assessment by the United Nations (UN) shows that approximately 68% of the global population will live in urban areas by 2050 [1]. Accompanying this trend, rapid concentration of urban population and economic activity drives intensive expansion of built-up areas. This process converts vast areas of natural vegetation into construction land or impervious surfaces, leading to habitat fragmentation, disruption of ecological processes, and reorganization of landscape patterns [2–4]. Vegetation loss directly caused by this land cover conversion is commonly recognized as the direct effect of urbanization on vegetation growth [5].

However, urbanization affects vegetation beyond spatial occupation alone. Existing research shows that urbanization also reshapes the thermal, hydrological, chemical, and management environments, producing more complex indirect effects on retained vegetation [6,7]. For example, urban heat islands alter surface energy balance and local temperature conditions, which in turn affect vegetation phenology, growing season length, and carbon assimilation [8,9]. Atmospheric pollutants, particularly ozone and particulate matter, weaken vegetation growth by inhibiting photosynthesis and damaging leaf tissues. Urban soil compaction, variations in physical and chemical properties, and altered water infiltration processes create persistent stress on root development and nutrient cycling [10–12]. Notably, moderate warming, elevated atmospheric CO_2 concentrations, and refined green space management may also promote urban vegetation through fertilization effects, extended growing seasons, and human compensation mechanisms [13–16]. Therefore, the ecological effects of urbanization on vegetation are not unidirectional suppression, but rather the net result of combined direct displacement and indirect regulation.

Urban vegetation serves as an important foundation of urban ecosystems. It plays an irreplaceable role in regulating microclimate, reducing thermal risk, maintaining biodiversity, and improving livability [17–20]. However, compared with direct effects, the indirect effects of urbanization often exhibit ecological lag and spatial heterogeneity, making them prone to being masked by short-term data and coarse-resolution analysis [21,22]. Most existing studies use Normalized Difference Vegetation Index (NDVI) or Enhanced Vegetation Index (EVI) to characterize vegetation responses and focus on discussing the overall impact of urban expansion on vegetation cover, vegetation phenology, or greenness change. Although these studies have yielded rich results, most remain at the level of overall associations or direct effects, with insufficient identification, separation, and quantification of indirect effects [23–25].

Further analysis reveals significant limitations in temporal dynamics and mechanistic explanation in existing research. Regarding temporal dynamics, existing studies rarely discuss differences between short-run and long-run effects. Concerning lag phenomena in vegetation responses to urbanization, most existing studies employ correlation analysis, conventional regression, or general causality testing. Although these can identify temporal lags in responses, they struggle to further distinguish between short-run impacts and long-run equilibrium effects [26–29]. In contrast, the Autoregressive Distributed Lag model (ARDL) and its error correction formulation can simultaneously estimate short-run fluctuations, long-run equilibrium relationships, and system adjustment speed within a cointegration framework. This provides a more explanatory analytical tool for identifying dynamic responses of vegetation systems under urbanization disturbance [30–32].

Nanjing is located in the western Yangtze River Delta and represents a typical rapidly urbanizing major city in eastern China. Between 2001 and 2018, Nanjing underwent a critical transition from lateral expansion to parallel ecological restoration and spatial optimization. The city exhibits significant expansion of built-up areas, population concentration, and three-dimensional spatial restructuring, providing an ideal study area for identifying the direct and indirect pathways of urbanization on vegetation growth and their short-run and long-run dynamics.

Building on this foundation, this study examines Nanjing through combined spatio-temporal analysis and the ZHAO conceptual model, isolating impervious surface effects from vegetation signals to focus on how urbanization indirectly regulates vegetation [33]. Methodologically, this study employs the CS-ARDL model, which has the advantage of simultaneously accounting for cross-sectional heterogeneity and cross-sectional dependence among samples [34]. The study decomposes the indirect effects of urbanization intensity on vegetation into short-run effects, long-run equilibrium effects, and error correction speed, with comparative analysis across different regions under different urban development stages [35]. By simultaneously characterizing long-run and short-run response characteristics, this study aims to answer

more clearly whether urbanization in different regions is more stimulating or more inhibitory to vegetation, and how this effect changes over time. The findings can provide more direct empirical reference for ecological space optimization and green space management in rapidly urbanizing regions.

2 Materials and Methods

2.1 Study Area Description

Nanjing is located in the western Yangtze River Delta region of China, belonging to a typical East Asian monsoon climate zone (Fig. 1). The study area is characterized by distinct seasons and abundant precipitation. The long-term mean annual temperature is 15.4°C, with an average annual rainfall of 1106.5 mm and a mean relative humidity of 76%. Overall, the climate is warm and humid. Between 2001 and 2018, the Nanjing region exhibited a significant warming trend, with winter warming being particularly pronounced. As the capital of Jiangsu Province, the core city of the Nanjing metropolitan area, and a major megacity in the East China region, it has long possessed favorable natural conditions and abundant vegetation. However, since economic reform and opening-up, Nanjing has undergone highly representative urban spatial expansion accompanying rapid industrialization and urbanization. Driven by the construction of typical industrial parks including Jiangning Economic Development Zone, Nanjing High-tech Industrial Development Zone (Pukou), Nanjing Economic and Technological Development Zone, and Nanjing Chemical Industrial Park, its permanent population increased rapidly from 5.45 million in 2000 to 9.31 million in 2020. During this process, the expansion pattern driven by newly built industrial parks and supporting residential areas led to large areas of natural vegetation and cultivated land being replaced by impervious surfaces, with some built-up areas developing contiguously, producing profound impacts on regional microclimate, carbon budget, and ecosystem functions. This transition pattern makes Nanjing an ideal site for studying how high-intensity urbanization drives long-run and short-run vegetation dynamics.

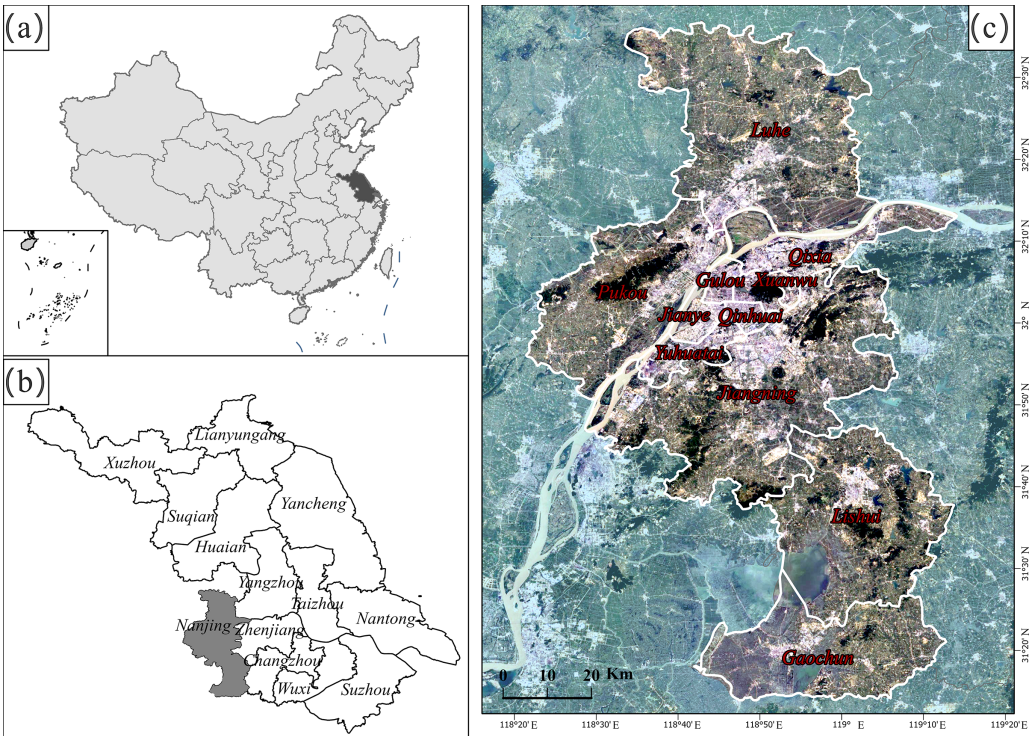

Figure 1: Study area. (**a**) China. (**b**) Jiangsu Province. (**c**) Nanjing Google RSI in 2020.

2.2 Data

This study constructed a panel dataset encompassing urbanization intensity, vegetation indices, and indirect effects. To ensure effective integration of multi-source raster data, all data were unified to the WGS-84 coordinate system unless otherwise specified. Data sources and processing methods are detailed below:

Urban Boundary and Analysis Grid: We used the multi-temporal Global Urban Boundary (GUB) dataset released by Professor Gong Peng's team at the Department of Earth System Science, Tsinghua University [36]. This dataset, derived from GAIA impervious surface data, precisely delineates global urban boundaries with areas exceeding 1 km^2. We extracted the urban boundaries of Nanjing for 2000 and 2018. Using the 2018 boundary as a reference, we created a buffer zone and established a 1 km spatial grid. To avoid the confounding effects of elevation and water bodies on vegetation growth, we excluded grid cells with elevation exceeding 50 m or containing water bodies. Accordingly, grid cells within the 2000 boundary were classified as "core urban areas". Grid cells in the expansion zone during 2000–2018 were classified as "suburban areas". Grid cells outside the 2018 boundary were classified as "rural areas".

Urbanization Intensity (UI): Urbanization intensity was characterized by the proportion of impervious surfaces (β), derived from the Global Artificial Impervious Area (GAIA) dataset released by Tsinghua University's team [37]. This dataset was produced from long-term Landsat time series, nighttime light data, and Sentinel-1 radar data, with overall accuracy exceeding 90%. It provides 30 m resolution impervious surface distributions globally from 1985 to 2018. Using spatial statistics, we calculated the proportion of impervious surface pixels within each 1 km grid cell to obtain annual urbanization intensity indicators.

Vegetation Index (VI): Vegetation growth status was assessed using the MODIS Collection 6.1 MOD13A2 product (1 km spatial resolution, 16-day composite temporal resolution) [38]. Compared to NDVI, EVI effectively mitigates interference from background soil and atmospheric aerosols, and exhibits greater sensitivity to high biomass areas. We employed the Maximum Value Composite (MVC) method to derive annual EVI values, thereby characterizing annual vegetation growth across Nanjing. Specifically, we integrated the 16-day MOD13A2 EVI composites into annual values by taking the maximum EVI within each calendar year (23 scenes per year).

2.3 Methods

We employed the conceptual framework proposed by ZHAO to quantify the "indirect effects" of urbanization on vegetation, and applied the CS-ARDL model to distinguish the short-run dynamics and long-run equilibrium effects of this indirect relationship.

2.3.1 Quantification of Indirect Effects of Urbanization on Vegetation

Following the conceptual framework defined by ZHAO et al., we quantified the impact of urbanization on vegetation growth as direct and indirect effects. Direct effects manifest as the process of impervious surfaces replacing natural land surfaces, indirect effects refer to the net effects of environmental changes such as urban heat island and pollution, as well as human management practices during urbanization, on vegetation growth. This study divided the study area into 1 km grid cells. The observed VI values are given by the following Eq. (1):

$$V_{obs} = (1 + \omega_o)(1 - \beta) V_v + \beta V_{nv} \quad (1)$$

where V_{obs} represents the observed VI values of pixels, which is influenced by urbanization intensity β (defined as the proportion of impervious surfaces within the grid cell). The overall urbanization effect on VI is denoted as ω_o. V_v is the background vegetation index, representing conditions unaffected by urbanization.

It is determined by the mean VI of all grid cells with urbanization intensity of 0 in the corresponding year. V_{nv} is the VI of fully urbanized pixels (representing impervious surface-filled areas). Due to data statistical constraints, V_{nv} in this study is determined by the minimum VI values of grid cells with $\beta \approx 1$ in the corresponding year.

$$V_{zi} = (1 - \beta) V_v + \beta V_{nv} \tag{2}$$

Eq. (2) represents the zero-impact line, which is affected only by changes in urbanization intensity. The theoretical VI, denoted as V_{zi}, is defined by the background vegetation index V_v and the impervious surface index V_{nv}.

The overall urbanization effect on VI comprises direct effects (ω_d) and indirect effects (ω). Direct effects are always negative and can be expressed as Eq. (3):

$$\omega_d = \frac{V_{zi} - V_v}{V_v} \times 100\% \tag{3}$$

Indirect effects (ω) can be quantified by comparing the observed vegetation index at pixels (V_{obs}) with the theoretical vegetation index on the zero-impact line (V_{zi}). The sign of ω indicates whether the urban environment exerts a net promotion or inhibition effect on vegetation, while the magnitude reflects the strength of the indirect effect. As shown in Eq. (4):

$$\omega = \frac{V_{obs} - V_{zi}}{V_{zi}} \times 100\% \tag{4}$$

2.3.2 CS-ARDL Model

Since ecosystems subject to urbanization disturbance typically exhibit temporal lags and self-adjustment processes, this study employs the Autoregressive Distributed Lag model (ARDL) and its corresponding Error Correction Model (ECM) to characterize the short-term responses and long-term equilibrium effects of urbanization intensity on vegetation indirect effects [31]. The study further estimates the adjustment speed at which the system converges toward long-term equilibrium. Within a panel framework, the Cross-Sectional ARDL (CS-ARDL) estimation strategy is adopted to control for cross-sectional dependence, heterogeneity, and endogeneity issues, thereby balancing short-term heterogeneity across spatial units with consistency in long-term relationships [38].

(1) Basic Model: CS-ARDL(p, q)

Assuming the maximum lag orders for urbanization intensity (UI) and indirect effects on vegetation (ω) are p and q, respectively, the ARDL(p, q) basic model for an individual grid cell can be expressed as follows:

$$\omega_{it} = \mu_i + \sum_{j=1}^{p} \lambda_{ij} \omega_{i,t-j} + \sum_{k=0}^{q} \delta_{ik} \beta_{i,t-k} + \sum_{l=0}^{s} \phi_{il} \overline{\omega_{t-l}} + \sum_{l=0}^{s} \gamma_{il} \overline{\beta_{t-l}} + \varepsilon_{it}$$

where $i = 1, \ldots, N$ represents cross-sectional units. $t = 1, \ldots, T$ represents time. $\overline{\Omega_t}$ and $\overline{\beta_t}$ denote the cross-sectional arithmetic mean values of ω and β across all units in period t. $\overline{\omega_t} = N^{-1} \sum_{i=1}^{N} \omega_{it}$, $\overline{\beta_t} = N^{-1} \sum_{i=1}^{N} \beta_{it}$, $s = \lfloor T^{1/3} \rfloor$, λ_{ij}, δ_{ik}, ϕ_{il}, γ_{il} are parameters to be estimated. ε_{it} is the random error term and μ_I is the individual fixed effect.

If a long-term cointegration relationship exists between variables, the CS-ARDL model can be transformed through mathematical equivalence into an Error Correction Model (ARDL-ECM) to distinguish short-term shocks, long-term equilibrium effects, and adjustment speed.

$$\Delta\omega_{it} = \phi_i\left(\omega_{i,t-1} - \theta_i\beta_{i,t-1}\right) + \sum_{j=1}^{p-1}\lambda_{ij}^{*}\Delta\omega_{i,t-j} + \sum_{k=0}^{q-1}\delta_{ik}^{*}\Delta\beta_{i,t-k} + \sum_{l=0}^{s}\phi_{il}\overline{\omega_{t-l}} + \sum_{l=0}^{s}\gamma_{il}\overline{\beta_{t-l}} + \varepsilon_{it}$$

where, $\theta_i = \dfrac{\sum_{k=0}^{q}\delta_{ik}}{1-\sum_{j=1}^{p}\lambda_{ij}}$, $\phi_i = -\left(1-\sum_{j=1}^{p}\lambda_{ij}\right)$.

The equation consists of two main components.

Long-term equilibrium and adjustment mechanisms. The long-term multiplier θ_I represents the long-term equilibrium effect of urbanization intensity on vegetation indirect effects. Φ_I is the Error Correction Term (ECT), representing the adjustment speed at which short-term disequilibrium converges toward long-term equilibrium. For a long-term stable cointegration relationship to exist, ϕ_I must be significantly negative. A larger absolute value of ϕ_I indicates faster response of the vegetation system to external disturbances and shorter convergence time to the new equilibrium state.

Short-term dynamic shocks. Λ_{ij}^{*} and δ_{ik}^{*} are short-term dynamic coefficients. δ_{ik}^{*} specifically represents the short-run indirect effects of urbanization on vegetation. These reflect the short-term fluctuations and lagged characteristics of the vegetation system when facing rapid changes in surface physical conditions in current or lagged periods.

For the specific panel estimation strategy, this study employs the Mean Group (MG) model and uses the Pooled Mean Group (PMG) model as a robustness check. The PMG model allows short-term dynamic responses to vary across grid cells but constrains long-term evolution patterns (θ_i) to remain consistent across all grid cells.

3 Results

3.1 Spatiotemporal Evolution Patterns of Urbanization and Vegetation

From 2001 to 2018, Nanjing's urban construction land continuously expanded along the Yangtze River axis. Radiating from the main city center in the south, the built-up area extended toward the northeast, southwest, and southern directions. On the northern bank of the Yangtze River, expansion was constrained by Laoshan Mountain and the river system, forming a strip-like pattern oriented southwest to northeast. Beyond the main city, suburban and small cluster development proceeded in parallel, creating a composite pattern of "core—corridor—clusters". The urban extent in 2018 expanded approximately 142.29% relative to 2001, reflecting rapid and directional expansion.

Staged urbanization intensity (UI) increments across three periods (2001–2007, 2007–2013, 2013–2018) showed persistent high values along the Yangtze River corridor and the Jiangning–Hexi–Jiangbei New Area (Fig. 2). Regions constrained by Laoshan Mountain and the river system exhibited low growth increments across all three stages, reflecting stable topographic and hydrological controls. Overall expansion boundaries align closely with transportation corridors.

Relative EVI changes were highly coupled with urbanization expansion, displaying a ring-like structure of "core decline—periphery increase" (Fig. 2). EVI consistently declined in newly built-up areas, while showing significant increases in the urban-rural transition zones and around ecological green spaces. Patterns remained stable across the three periods, characterizing coexistence of negative effects at urbanization frontiers and positive feedbacks in peripheral areas.

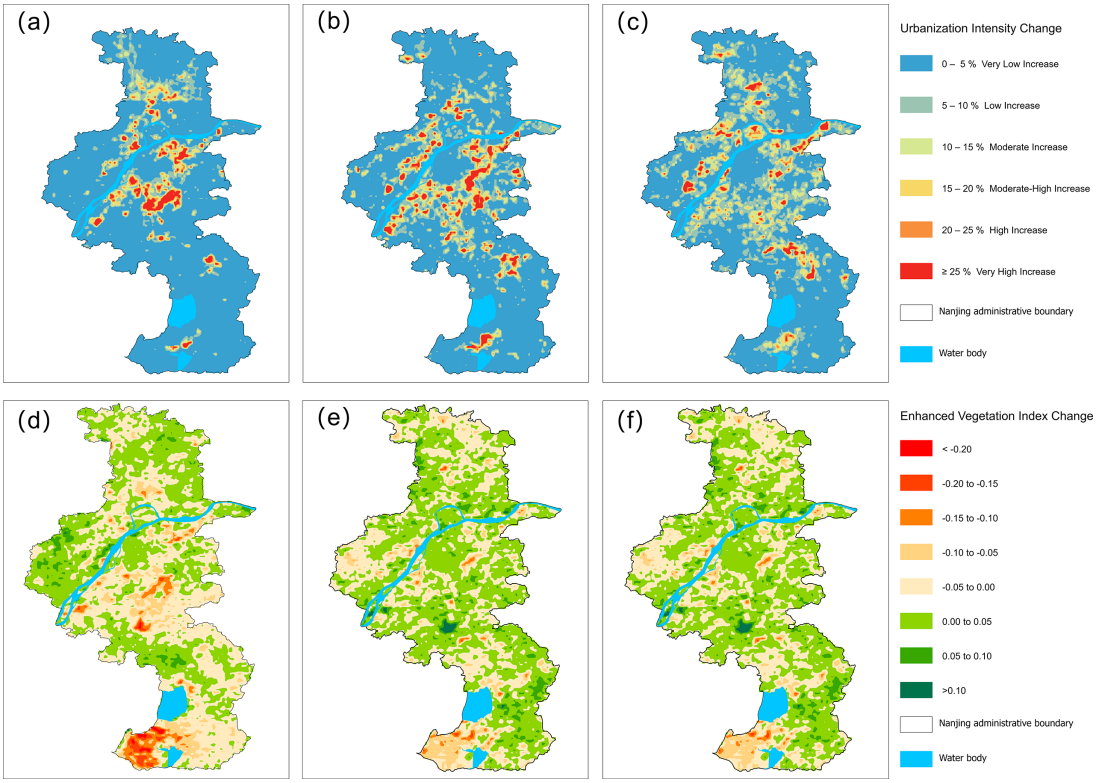

Figure 2: Spatial patterns of period-specific changes of urbanization intensity (UI) and vegetation index (EVI) in Nanjing from 2001 to 2018. (**a**–**c**) Mean annual rates of change in urbanization intensity (UI): (**a**) 2001–2006, (**b**) 2007–2012, (**c**) 2013–2018. (**d**–**f**) Concurrent changes in vegetation index (EVI): (**d**) 2001–2006, (**e**) 2007–2012, (**f**) 2013–2018. All values represent the mean annual rate of change (year^{-1}) within each period. The gray shading indicates the administrative boundary of Nanjing. Positive values indicate increase, negative values indicate decrease.

Established built-up areas, particularly core urban districts such as Xuanwu, Qinhuai, and Jianye districts, showed overall EVI increases. This suggests that at the stage when urbanization becomes stable, investments in green space construction, maintenance management, and tree species renewal, coupled with improved landscape connectivity, can partially offset negative impacts from impervious surface expansion.

In summary, Nanjing exhibited dual effects during the study period. In the urbanization expansion phase, newly added impervious surfaces triggered short-term EVI decline through thermal and water stress as well as habitat fragmentation. In the urbanization stabilization phase, intensified management and extended phenology drove EVI recovery and formed a positive anomaly zone at the periphery. This spatiotemporal combination reveals a stage-dependent mechanism where negative effects at expansion frontiers coexist with positive effects in stable built-up areas and surrounding buffer zones.

3.2 Spatiotemporal Evolution of Indirect Effects of Urbanization on Vegetation

Maps of indirect effects across three periods (Fig. 3) reveal distinct north-south spatial differentiation in how urbanization affects vegetation indirectly in Nanjing. Luhe District north of the Yangtze River exhibits a pronounced cluster of negative indirect effects. This indicates that vegetation in this region faces pressures far beyond direct encroachment from impervious surfaces. In contrast, urban core areas south of the Yangtze River (such as Xuanwu, Qinhuai, and Jianye districts) generally show positive indirect effects. More pronounced clusters of positive indirect effects appear within core urban districts. Positive indirect

effects suggest that urbanization in these areas is more likely to promote vegetation growth. The sign of indirect effects reflects the ecological orientation of urbanization. Positive ω indicates that urbanization has a positive promoting effect on vegetation growth, while negative ω indicates that urbanization exerts negative stress on vegetation. This spatial variation carries important practical implications. Luhe District is an important industrial base for Nanjing. The negative indirect effects likely reflect sustained vegetation stress from pollution emissions and possible lags in green space construction relative to urban expansion. Vegetation thus faces both direct encroachment and environmental pressure simultaneously. By contrast, positive indirect effects are more concentrated in core urban areas south of the Yangtze River. This result indicates that central districts have implemented more effective management and ecological construction measures. Urbanization may promote vegetation growth conditions by enhancing green infrastructure levels and strengthening ecological planning capacity.

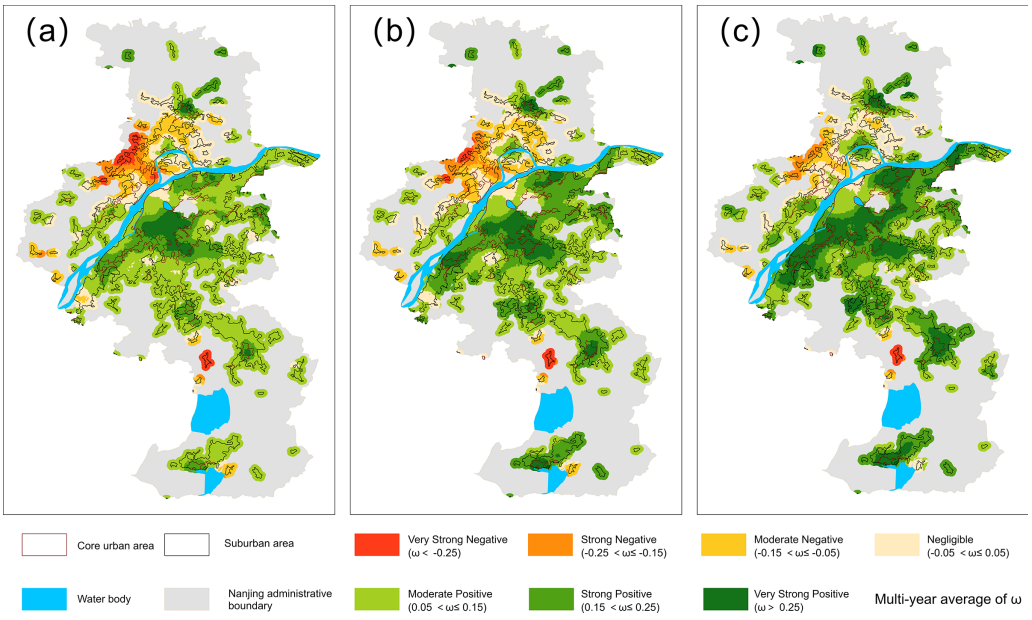

Figure 3: Spatial distribution of the indirect effects (ω) in Nanjing across three periods: (**a**) period-mean values for 2001–2006, (**b**) period-mean values for 2007–2012, and (**c**) period-mean values for 2013–2018. Values are classified into seven categories: Very Strong Negative (< −0.25), Strong Negative (−0.25 to −0.15), Moderate Negative (−0.15 to −0.05), Negligible (−0.05 to 0.05), Moderate Positive (0.05 to 0.15), Strong Positive (0.15 to 0.25), and Very Strong Positive (>0.25).

From 2001 to 2018, the indirect effects of urbanization on vegetation in Nanjing showed a systemic trend toward positive transformation. Negative indirect effects in Luhe District gradually eased. The dominant effect category shifted progressively from very strong negative to strong negative, further transitioning to weak moderate and negligible effects by 2013–2018. The proportion of strong negative areas declined significantly, reflecting weakening pressure on vegetation. Southern regions showed a trend of strengthening positive indirect effects. Positive indirect effects in core districts strengthened continuously, with dominant categories upgrading from strong positive to very strong positive. The strengthening of positive indirect effects suggests that ecological management and green space construction effectiveness in central districts may be deepening.

These changes collectively reflect a fundamental shift in Nanjing's urbanization trajectory. The weakening of negative indirect effects in industrial areas coincided with strengthening of positive indirect effects in core urban areas. Results indicate that urban development gradually transitioned from an expansion-dominated pathway toward an ecology-oriented approach. Within this context, vegetation is no longer merely a passive carrier for urban expansion. It increasingly becomes a priority object for urban greening and ecological protection. Simultaneously, Nanjing's sustained efforts in pollution control and ecological construction may have provided more stable environmental conditions for vegetation growth.

3.3 CS-ARDL Model Results Analysis

Before conducting panel ARDL model estimation, we first tested the stationarity of the grid panel data. Since spatial synchronization effects and spillover effects may exist among grid cells, we performed a Pesaran CD test. Results showed CD statistics of 5051.72 for β and 1000.03 for ω (both $p < 0.01$), indicating significant cross-sectional dependence. Therefore, we combined the traditional Fisher-ADF test with the CIPS test, which controls for cross-sectional dependence, to ensure robustness. The critical values for the CIPS test at 1%, 5%, and 10% significance levels are −2.63, −2.21, and −2.02, respectively. Results show that urbanization intensity (β) has a level series statistic of −1.227, exceeding the critical value of −2.02, which fails to reject the null hypothesis of a unit root. Its first differenced series statistic is −2.909 < −2.63, rejecting the null hypothesis and indicating first-order integration I(1). Indirect effects (ω) have a level series statistic of −3.102 < −2.63, indicating a stationary I(0) series. Both variables have orders of integration not exceeding 1, satisfying ARDL model prerequisites.

Based on confirmed stationarity at the same order, we conducted a panel cointegration test using the Kao residual-based approach to verify the long-run equilibrium relationship between variables. The Kao-type Fisher-ADF statistic reached 7389.21 ($p < 0.01$), strongly rejecting the null hypothesis of no cointegration. Additionally, Error Correction Model (ECM) estimation results show that error correction terms (ECT) are significantly negative at the 1% level across both the full sample and all sub-regions (the t-value of mean ECT for the full sample is −3.35, with over 90% of grid cells having significantly negative ECT). This further confirms an extremely stable long-run cointegrating relationship between urbanization intensity (β) and indirect effects (ω) that converges toward equilibrium, providing a reliable econometric foundation for subsequently decomposing short-run and long-run effects using MG/PMG estimation.

3.3.1 Short-Run and Long-Run Dynamic Heterogeneity of Indirect Effects

We selected the optimal lag order based on AIC and BIC information criteria. Within the maximum lag order range (p = 2, q = 2), both AIC and BIC values for the full sample and all sub-regions supported CS-ARDL(1, 1) as the optimal model. To choose between MG and PMG estimation, we performed a Hausman test with the null hypothesis of homogeneous long-run coefficients (PMG consistency). Full sample test results showed χ^2 (1) = 11,411.61 with $p < 0.01$, rejecting the null hypothesis of homogeneous long-run coefficients. Thus, the MG model is statistically more appropriate, and we use it as our primary model for subsequent interpretation (see Table 1). After obtaining estimates, we tested for spatial autocorrelation in residuals using Moran's I. Results showed Moran's I = −0.0256 with $p = 0.074$, indicating no significant spatial autocorrelation at the residual level, which is consistent with the model's mitigation of spatial dependence. Given that individual grid cell time series are short (T = 18), information criteria based on single samples (such as BIC) may underestimate lag orders due to severe parameter penalties. Since both AIC and BIC values support CS-ARDL(1, 1) as optimal across the full sample and all sub-regions, we adopt a uniform ARDL(1, 1) specification at the grid scale to ensure consistent parameter extraction across regions.

In the long-run equilibrium state, the system exhibits strong self-correction capacity and positive long-run effects. The full sample ECT coefficient is −1.051, indicating that when the system deviates from equilibrium, it adjusts toward equilibrium at a rate of λ = 1.051. The adjustment half-life, approximated by $\ln 2/\lambda$, is about 0.66 years, reflecting a rapid convergence process. Across the full sample, urbanization intensity (β) and resulting indirect effects (ω) show overall positive long-run effects (0.423), consistent with existing research finding widespread positive indirect effects of urbanization on vegetation. From a spatial gradient perspective, long-run positive effects display a distinct pattern: core urban areas (1.963) > suburban areas (0.373) > rural areas (−0.149). Core urban areas exhibit the strongest and largest long-run effects, suburban areas are positive but with smaller magnitude, while rural areas are negative. Compared to the insignificant long-run effects observed in both the full sample and rural areas, this may reflect intra-regional heterogeneity, statistical imprecision from spatial scale aggregation, or instability in long-run relationships. Presenting these spatial differences through maps aids more accurate interpretation of spatial heterogeneity under MG estimation.

In short-run dynamic response, sub-regions display more pronounced heterogeneity. Core urban areas show high short-run effects (0.509). Vegetation responds more sensitively to urbanization intensity fluctuations in the short term. This may reflect stronger and more synchronized ecological management in these areas, providing immediate support for short-term vegetation recovery. Suburban areas display short-run effects near zero. This possibly reflects time-lag or staged adaptive responses of ecosystems to urban expansion away from core conservation areas. Rural areas show positive short-run effects that turn negative in the long run. This suggests short-term positive changes may not persist. They ultimately manifest as negative results in long-run equilibrium. Regarding significance, we refer to significance levels of MG short-run coefficients in Table 1. Overall, short-run effects are less stable. This indicates that urbanization impacts on vegetation may exhibit fluctuating characteristics in the short term due to multiple staged factors.

Table 1: Regional panel CS-ARDL estimation results of the indirect impacts of urbanization on vegetation.

Sample Regions	Model	Long-Run Effect (θ)	Short-Run Effect (δ_i)	ECT (ϕ_i)	Selection
Full Sample	MG	+0.423 (0.301)	+0.231 (0.158)	−1.051*** (0.007)	MG
	PMG	+0.269*** (0.046)	+0.366*** (0.105)	−0.919*** (0.007)	
Core Urban	MG	+1.963* (1.158)	+0.509 (0.826)	−0.975*** (0.017)	MG
	PMG	+0.037* (0.665)	+1.089 (0.545)	−0.886*** (0.018)	
Suburban	MG	+0.373*** (0.019)	+0.009 (0.044)	−0.936*** (0.010)	MG
	PMG	+0.348*** (0.025)	+0.117*** (0.043)	−0.936*** (0.010)	
Rural	MG	−0.149 (0.260)	+0.157 (0.148)	−1.061*** (0.010)	MG
	PMG	+0.298*** (0.073)	−0.077 (0.130)	−1.009*** (0.010)	

Note: ***, * denote statistical significance at the 0.01, and 0.1 levels, respectively; figures in parentheses are standard errors.

3.3.2 Spatial Microscale Characteristics of Long-Run Equilibrium Effects

To further reveal spatial heterogeneity at the grid-cell scale, we conducted independent ARDL estimates for each grid cell under a unified lag specification. Results show that short-run effects attained statistical significance in fewer than 30% of grid cells. This pattern is consistent with the overall instability and weak significance of short-run coefficients in MG estimation.

The fundamental reason lies in the short time series length (18 years per grid cell). This limits statistical power and increases exposure to random fluctuations. Additionally, the error correction term (ECT) reflects rapid convergence speed. Deviations from long-run equilibrium are strongly corrected in subsequent years. This makes it more difficult to reliably identify short-run net effects at the individual grid-cell level on an annual basis. Local management differences and environmental disturbances may further dampen short-run signals.

By contrast, long-run equilibrium effects demonstrate higher consistency and comparability in grid-cell level estimates. Long-run relationships rely on cumulative temporal information. They are typically less sensitive to short-term noise than short-run effects. Even if individual grid cells fail significance tests due to data fluctuations, their parameter estimates remain spatially comparable.

Overall, long-run effects (Fig. 4) reveal significant positive impacts across most areas. However, notable clusters of negative effects appear locally. One location is within core urban areas. Scattered negative-effect patches appear in central Qinhuai District, central Gulou District, the boundary between Jianye and Gulou Districts, and far western Qixia District. These areas have very high proportions of impervious surfaces. Available space and means for artificial vegetation enhancement have reached practical limits. Soil compaction, constrained root development, and microclimatic heat stress make it difficult to further improve vegetation quality even with fine management. The marginal benefits of indirect effects have been exhausted.

At the expanding outer suburban fringe, we observe effect reversals across the urban-rural gradient. Suburban areas are predominantly characterized by stable positive effects. The transitional zone toward rural areas exhibits emerging negative trends in some grid cells. The area south of Laoshan in Pukou District is most typical, forming a distinct cluster of negative effects. Urban margins of Jiangning, Lishui, and Gaochun also show negative trends, but their patterns display more pronounced interspersion of positive and negative values with weaker spatial continuity. Luhe District's suburban fringe and urban core areas are primarily dominated by positive effects. These spatial differences may relate to variations in development pace, timing of management investments, and baseline ecological conditions across different areas.

4 Discussion

This study characterizes the indirect effects of urbanization on vegetation in Nanjing from two dimensions: spatiotemporal evolution and long-run/short-run effects. Overall, the sustained outward expansion of urban construction land along the Yangtze River axis and the "core-corridor-cluster" expansion pattern provide a stable spatial background for vegetation response. Meanwhile, the EVI maps across the three periods reveal a ring-like structure characterized by "core decline and peripheral rise," suggesting that urbanization at different stages and locations may correspond to ecological consequences with opposite directions. This characteristic provides intuitive foundation for interpreting the long-run and short-run differences in dynamic econometric analysis.

The spatial distribution of indirect effects across the three periods (Fig. 3) displays pronounced north-south divergence. Areas north of the Yangtze River (represented by Luhe District) are more prone to negative indirect effect clustering. In contrast, the urban core south of the Yangtze River generally tends toward positive indirect effects, with positive clustering within the core urban areas being relatively more concentrated. This north–south contrast is broadly consistent with the compensatory urban–suburban gradient reported in a multi-city NDVI study (2000–2020), where compensation strength follows old urban areas > new urban areas > suburbs [39]. Accordingly, Nanjing's developmental structure—northward largely corresponding to new/edge urbanization and the south hosting the older core—may help explain why negative tendencies dominate the north while compensatory (positive) indirect effects are more evident in the southern core.

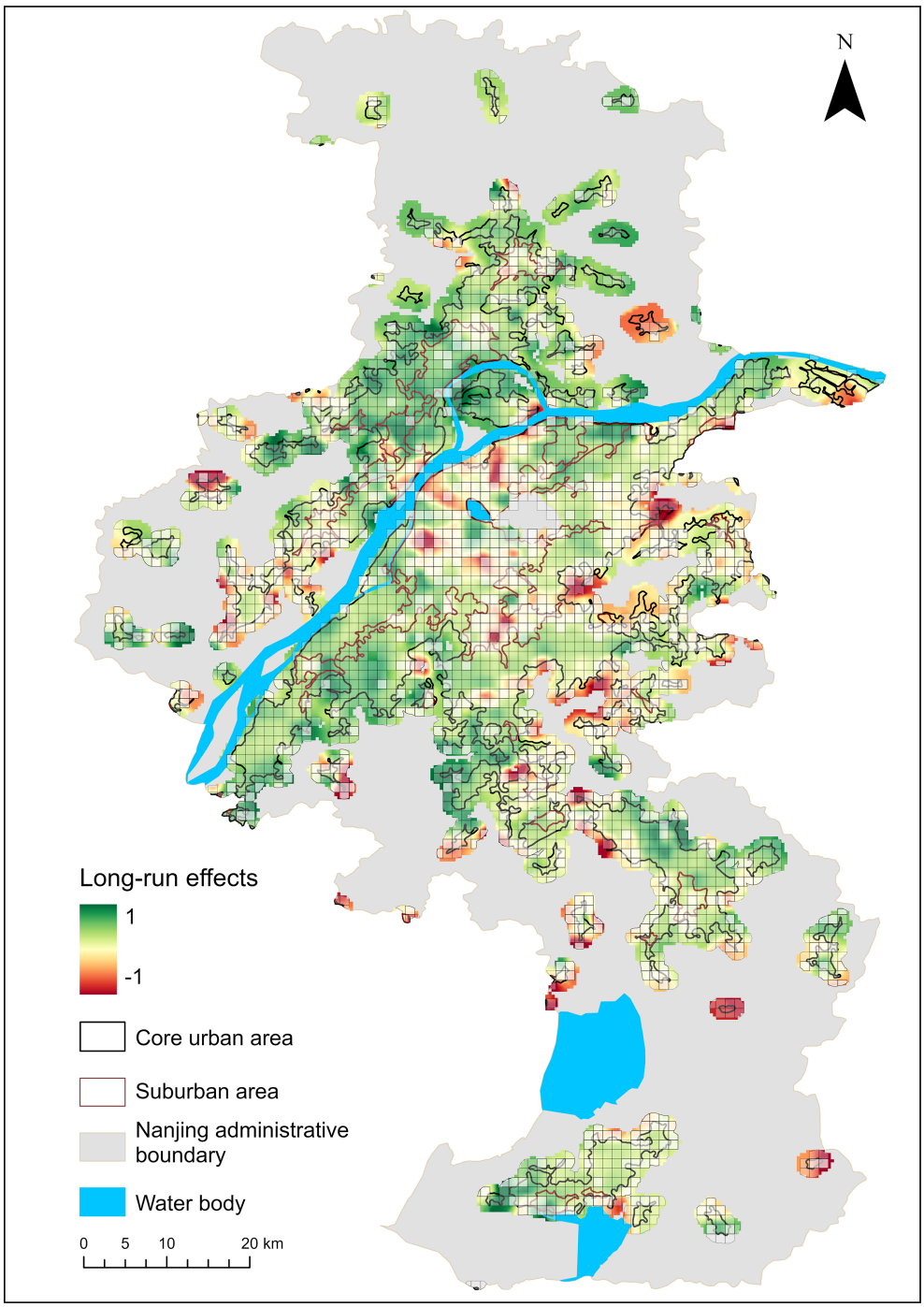

Figure 4: Spatial distribution of long-run equilibrium effects of urbanization on vegetation indirect impacts. Pixel values represent long-run effect coefficients estimated by CS-ARDL. Positive values (green) and negative values (red) respectively indicate long-run positive enhancement and negative suppression effects. White semi-transparent masked areas represent grid cells that fail to pass the 10% significance test ($p > 0.1$).

This pattern of "negative tendency in the north, positive tendency in the south" likely relates to regional environmental pressure and governance rhythm. For areas north of the Yangtze River, the region (particularly southern Luhe District) historically concentrated substantial heavy chemical industries. Taking the Dachang

area in Jiangbei New Area as an example, it was once one of Nanjing's most concentrated old industrial bases. Long-term operation of major chemical enterprises such as Nanjing Chemical Company accumulated prominent environmental problems. By 2013, the four major areas including Jinling Petrochemical, Dachang, Meishan Steel, and Yangtze River waterfront collectively covered approximately 112.6 square kilometers and concentrated over one hundred chemical and steel enterprises. Nanjing Chemical Company was even restricted by the Nanjing Environmental Protection Bureau from developing new projects due to failure to complete pollutant reduction targets in the 11th Five-Year Plan. Simultaneously, heavy chemical industries clustered in the chemical industrial park in southern Luhe. Pollutant emissions and energy consumption represented a major share of the municipal total, placing Luhe District under sustained high environmental pressure. Against this background, vegetation was more likely to display negative response to the indirect effects of urbanization. Additionally, temporal misalignment between new expansion and greenery construction or maintenance investment may have occurred. This could amplify negative signals near expansion boundaries due to "greenery functions not yet fully realized." However, it is worth noting that, with the strengthening of environmental management efforts in the Jiangbei area, the potential external pressures on vegetation in this region may have been alleviated over time.

However, it is noteworthy that as environmental management in the Jiangbei area has progressively strengthened, the external pressures acting on vegetation in this region may have been alleviated over time. The Jiangbei area, especially southern Luhe District, historically concentrated numerous heavy and chemical industries. The Dachang industrial zone, located in northern Jiangbei, exemplifies this legacy. Once the most concentrated old industrial base in Nanjing, it accumulated substantial environmental problems from long-term operations of large-scale petrochemical enterprises such as Nanhua Chemical Company. By 2013, the "Four Major Industrial Clusters" region—including Jinling Petrochemical, Dachang, Meishan Steel, and areas along the Yangtze River—covered approximately 112.6 square kilometers and concentrated over one hundred chemical and steel enterprises. The environmental pressure was severe: Nanhua Chemical Company was even restricted from new project development by Nanjing Environmental Protection Bureau due to failure to complete pollution reduction targets in the 11th Five-Year Plan period.

Southern Luhe District's chemical industrial park further concentrated heavy chemical enterprises. Pollutant emissions and energy consumption accounted for a disproportionate share of the city's total, subjecting the district to persistently high environmental stress. Under these circumstances, vegetation growth may be constrained, which could be one of the reasons for the observed negative indirect effects of urbanization on vegetation in this region. Additionally, temporal misalignment between new development expansion and greening investment may have amplified negative signals, as green space functions had not yet fully developed at expansion boundaries.

However, it is noteworthy that as Nanjing progressively intensified environmental management efforts in the Jiangbei region. This may have contributed to alleviating the environmental pressures on vegetation growth in this region. In 2013, Nanjing explicitly required restructuring of industrial and energy structures, implementing strict environmental access standards. The city prohibited new construction or expansion of high-pollution projects in coal-fired power generation, steel, and cement sectors, and enforced national industrial policies and environmental standards rigorously. Efforts to phase out outdated production capacity in chemical and metallurgical industries were significantly strengthened. That same year, Luhe District incorporated the closure and renovation of 187 boilers into its annual plan.

In 2014, Nanjing launched the "Four Major Industrial Clusters" industrial restructuring plan. This plan aimed to relocate and upgrade key energy-intensive enterprises in Jinling Petrochemical, Meishan Steel, and Dachang areas over approximately ten years. Notably, the Dachang area in northern Jiangbei was included in the national old industrial base revitalization program, with explicit plans to gradually close Nanhua

Chemical and Nanggang Steel and other key energy-intensive enterprises. Simultaneously, strict controls were placed on new industrial projects. These successive measures have gradually reduced pollution in the northern Jiangbei region, which may help explain the spatial contraction and attenuation of the negative indirect effects of urbanization on vegetation growth observed in this area.

By contrast, the core urban area south of the Yangtze River likely benefited from earlier initiation and more systematic ecological governance coupled with refined green space maintenance. From a policy perspective, Nanjing has progressively strengthened its institutional framework for green space construction and ecological management around the theme of "green development."

As early as 2002, Nanjing released the Opinion on Building "Green Nanjing", establishing dedicated subsidy funds for green development and launching the "Green Metropolis" construction initiative. Subsequently, large-scale greening and afforestation campaigns were implemented. By 2006, the Master Plan for Nanjing Ecological City Construction was released, designating seven core green lines including Zijin Mountain and Laoshan. In 2011, the Interim Measures for Urban Green Line Management in Nanjing was issued and implemented, further establishing a mandatory control system for various urban green spaces. In 2013, the Urban Greening Ordinance of Nanjing officially took effect. The 2018 Working Plan for Creating a National Ecological and Garden City in Nanjing set even higher standards. The plan specified concrete targets such as achieving a green space rate of 40.75% in the urban built-up area and per capita park green space of 15.5 m^2.

Concurrently, the "Green Nanjing" strategy continued to advance through large-scale afforestation campaigns. Over twenty years, Nanjing cumulatively afforested more than 90,700 km^2, and protective forests spanning approximately 6700 km^2 along both sides of the Yangtze River gradually formed a continuous and intact green ecological corridor. Based on these efforts, Nanjing was successfully recognized as a "National Forest City" in 2018. The core urban area south of the Yangtze River developed within this series of policy-guided green space construction, sustained management investment, and landscape connectivity improvements. This may partially account for the increase observed over the past 18 years in the indirect effects of urbanization on vegetation growth in the Nanjing region.

The CS-ARDL model results further demonstrate that urbanization's indirect effects on vegetation in Nanjing exhibit characteristics of "long-run positive robustness coupled with short-run heterogeneous fluctuations."

At the long-run equilibrium level, the long-run coefficients are generally positive, spatially exhibiting a declining gradient of "core urban areas > suburban areas > rural areas." Notably, the rural long-run effect is negative but not statistically significant (or exhibits instability across sub-regions). This suggests that rural areas may harbor stronger process heterogeneity and measurement noise, or may reflect limitations in identifying long-term relationships at the aggregated level.

At the short-run dynamic level, sub-regions display more pronounced heterogeneity. Core urban areas exhibit stronger short-run responses, whereas suburban and rural areas may show weak responses or lagged characteristics at different stages. Meanwhile, the statistical significance of short-run effects is relatively fragile. This does not necessarily indicate the absence of short-term mechanisms; rather, it more likely reflects that annual-scale vegetation changes are subject to multiple concurrent disturbances (such as meteorological year-to-year fluctuations, management activity variations, and surface process volatility). These disturbances likely reduce the identifiability of the urbanization variable on indirect effects, rather than negating the true short-term response.

At finer scales, the grid-cell long-run effect maps reveal localized clusters of negative effects, appearing in both core urban areas and expanding suburban margins. These findings suggest that within these regions, the

long-run equilibrium effects of urbanization on indirect impacts are likely to be weaker or less favorable. The specific sources remain open to interpretation. Potential mechanisms include impervious surface pressure, thermal and water environment disturbances, habitat fragmentation, and temporal misalignment between management investments and ecological processes. For now, these should be treated as candidate explanations and expressed with appropriate caution. Future work will need to validate them by incorporating variables with stronger process orientation.

Overall, ecological effects at longer time scales show greater stability and clearer spatial gradients. At shorter time scales, results are more constrained by temporal information limits and process heterogeneity, causing statistical significance to be more easily diluted. Accordingly, management strategies should balance two priorities. First, they must consolidate long-run ecological gains. Second, they should identify which regions and time periods face short-run disturbances that may prove resistant to rapid correction. This assessment should support differentiated management practices tailored to specific zones and phases, alongside sustained monitoring efforts.

This study employs the CS-ARDL approach to decompose the indirect effects of urbanization on vegetation growth into short-run dynamics and long-run equilibrium components. By doing so, it may help mitigate the influence of short-term shocks on the estimation of the underlying long-term relationship. This framework therefore supports a clearer understanding of how vegetation responses evolve toward a more stable state following urban expansion. However, CS-ARDL relies on sufficiently long time series for reliable estimation, and its performance may be constrained when the available temporal span is relatively limited.

While this study characterizes the spatiotemporal variations in the indirect effects of urbanization on vegetation growth, it does not explicitly disentangle the mechanisms responsible for these patterns. Future research will therefore extend the modeling framework by incorporating plausible mediating factors—such as management inputs, pollution loads, and extreme climate indicators—to identify the drivers underlying the persistence and formation of negative-effect clustering areas. In addition, Future research will also use longer time series and more process-based indicators to further distinguish short-term disturbances from subsequent vegetation responses, thereby improving the temporal interpretability and readability of the results.

5 Conclusions

This study examined the indirect ecological effects of urbanization on vegetation based on a framework analyzing spatial-temporal evolution and short-run vs. long-run dynamics from 2001 to 2018 in Nanjing. Using CS-ARDL and error correction methodology, we decomposed long-run equilibrium effects, short-run shock responses, and system adjustment characteristics. The results show that urban construction land expanded continuously along the Yangtze River axis, forming a "core–corridor–cluster" spatial pattern. Indirect vegetation impacts exhibited pronounced north-south differentiation: areas north of the Yangtze (such as Luhe District) experienced negative clustering, while the core urban area south of the Yangtze showed overall positive responses with an evolutionary pattern of "negative–weak negative–shift to positive" during the study period. ARDL results further revealed that at the long-run scale, urbanization's indirect effects on vegetation were predominantly positive, displaying a declining gradient from "core urban areas > suburban areas > rural areas." The short-run scale demonstrated stronger spatial heterogeneity and volatility. The system-level error correction term was consistently negative, indicating strong adjustment capacity when deviating from long-run equilibrium. However, localized negative clustering zones signal ecological vulnerability risks. For policy implications, the study supports consolidating long-run ecological gains while implementing differentiated, stage-specific fine-grained green space management and continuous monitoring in regions with pronounced short-run fluctuations. Future work should introduce variables

capturing management investment, pollution, extreme climate events, and surface processes to verify the drivers underlying negative clustering patterns.

Acknowledgement: Not applicable.

Funding Statement: This work is supported by the Major Program of the National Natural Science Foundation of China (Grant No. 42230113).

Author Contributions: Xiankai Ji: Writing—original draft, Writing—review & editing, Software, Methodology, Formal analysis, Conceptualization. Manchun Li: Writing—review & editing, Data curation, Methodology, Investigation, Funding acquisition, Conceptualization. Nan Xia: Writing—review & editing, Methodology, Supervision, Formal analysis, Conceptualization. All authors reviewed and approved the final version of the manuscript.

Availability of Data and Materials: The data that support the findings of this study are available from the Corresponding Author, Manchun Li, upon reasonable request.

Ethics Approval: Not applicable.

Conflicts of Interest: The authors declare no conflicts of interest.

References

1. UN Department of Economic and Social Affairs. World urbanization prospects: the 2018 revision. New York, NY, USA: DESA UN; 2019.
2. Korah A, Wimberly MC. Annual impervious surface data from 2001–2020 for west African countries: Ghana, Togo, Benin and Nigeria. Sci Data. 2024;11(1):791. doi:10.1038/s41597-024-03610-8.
3. Carlson TN, Traci Arthur S. The impact of land use—land cover changes due to urbanization on surface microclimate and hydrology: a satellite perspective. Glob Planet Change. 2000;25(1–2):49–65. doi:10.1016/S0921-8181(00)00021-7.
4. Zhong J, Tu J, Li X, Fu Y, Liu W, Zhang F, et al. Variation in vegetation characteristics and landscape patterns of urban forests: implications for ecosystem management under rapid urbanization. J For Res. 2025;36(1):123. doi:10.1007/s11676-025-01921-z.
5. Yin C, Xiao X, Pan L, Chen R, Yin Y, Qin Y, et al. Concurrent increases of impervious surface area and vegetation greenness and productivity in China's Yangtze River Delta. Earth's Future. 2025;13(12):e2025EF006652. doi:10.1029/2025ef006652.
6. Zhang L, Yang L, Zohner CM, Crowther TW, Li M, Shen F, et al. Direct and indirect impacts of urbanization on vegetation growth across the world's cities. Sci Adv. 2022;8(27):eabo0095. doi:10.1126/sciadv.abo0095.
7. Jia W, Zhao S, Zhang X, Liu S, Henebry GM, Liu L. Urbanization imprint on land surface phenology: the urban-rural gradient analysis for Chinese cities. Glob Chang Biol. 2021;27(12):2895–904. doi:10.1111/gcb.15602.
8. Zhou D, Zhao S, Zhang L, Liu S. Remotely sensed assessment of urbanization effects on vegetation phenology in China's 32 major cities. Remote Sens Environ. 2016;176:272–81. doi:10.1016/j.rse.2016.02.010.
9. Wang J, Xiang Z, Wang W, Chang W, Wang Y. Impacts of strengthened warming by urban heat island on carbon sequestration of urban ecosystems in a subtropical city of China. Urban Ecosyst. 2021;24(6):1165–77. doi:10.1007/s11252-021-01104-8.
10. Lapina K, Henze DK, Milford JB, Travis K. Impacts of foreign, domestic, and state-level emissions on ozone-induced vegetation loss in the United States. Environ Sci Technol. 2016;50(2):806–13. doi:10.1021/acs.est.5b04887.
11. Das TK, Kabir A, Zhao W, Stenstrom MK, Dittrich TM, Mohanty SK. A review of compaction effect on subsurface processes in soil: implications on stormwater treatment in roadside compacted soil. Sci Total Environ. 2023;858(3):160121. doi:10.1016/j.scitotenv.2022.160121.

12. Zhang P, Dong Y, Guo Y, Wang C, Wang G, Ma Z, et al. Urban forest soil is becoming alkaline under rapid urbanization: a case study of Changchun, Northeast China. Catena. 2023;224:106993. doi:10.1016/j.catena.2023.106993.
13. Mu W, Zhu X, Ma W, Han Y, Huang H, Huang X. Impact assessment of urbanization on vegetation net primary productivity: a case study of the core development area in central Plains urban agglomeration. China Environ Res. 2023;229(1):115995. doi:10.1016/j.envres.2023.115995.
14. Rezende LFC, de Castro AA, Von Randow C, Ruscica R, Sakschewski B, Papastefanou P, et al. Impacts of land use change and atmospheric CO_2 on gross primary productivity (GPP), evaporation, and climate in southern Amazon. J Geophys Res Atmos. 2022;127(8):e2021JD034608. doi:10.1029/2021jd034608.
15. Nizamani MM, Harris AJ, Cheng XL, Zhu ZX, Jim CY, Wang HF. Positive relationships among aboveground biomass, tree species diversity, and urban greening management in tropical coastal city of Haikou. Ecol Evol. 2021;11(17):12204–19. doi:10.1002/ece3.7985.
16. Du C, Ge S, Song P, Jombach S, Fekete A, Valánszki I. Optimizing urban green spaces for vegetation-based carbon sequestration: the role of landscape spatial structure in Zhengzhou Parks. China Forests. 2025;16(4):679. doi:10.3390/f16040679.
17. Priya UK, Senthil R. A review of the impact of the green landscape interventions on the urban microclimate of tropical areas. Build Environ. 2021;205(3):108190. doi:10.1016/j.buildenv.2021.108190.
18. Twohig-Bennett C, Jones A. The health benefits of the great outdoors: a systematic review and meta-analysis of greenspace exposure and health outcomes. Environ Res. 2018;166:628–37. doi:10.1016/j.envres.2018.06.030.
19. Veerkamp CJ, Schipper AM, Hedlund K, Lazarova T, Nordin A, Hanson HI. A review of studies assessing ecosystem services provided by urban green and blue infrastructure. Ecosyst Serv. 2021;52(3):101367. doi:10.1016/j.ecoser.2021.101367.
20. Jovanović S, Janković-Milić V, Stanković JJ, Stanojević M. The role of urban tree areas for biodiversity conservation in degraded urban landscapes. Land. 2025;14(9):1815. doi:10.3390/land14091815.
21. Yin P, Li X, Zhou Y, Mao J, Fu YH, Cao W, et al. Urbanization effects on the spatial patterns of spring vegetation phenology depend on the climatic background. Agric For Meteor. 2024;345(1):109718. doi:10.1016/j.agrformet.2023.109718.
22. Zhang S, Zhu H, Zeng K, Zhang Y, Jin Z, Wang Y, et al. From city to countryside: unraveling the long-term complex effects of urbanization on vegetation growth in China. J Environ Manag. 2025;380:124975. doi:10.1016/j.jenvman.2025.124975.
23. You YJ, Liu M, Ni HG. Dynamic indirect impacts of urbanization on vegetation growth in Chinese cities. Int J Appl Earth Obs Geoinf. 2024;131:103974. doi:10.1016/j.jag.2024.103974.
24. Peng L, Huang K, Zhang H, Sun W. Exploring the impacts of urbanization on vegetation growth from the perspective of urban expansion patterns and maturity: a case study on 40 large cities in China. Sustain Cities Soc. 2024;115(9):105841. doi:10.1016/j.scs.2024.105841.
25. Zhu E, Fang D, Chen L, Qu Y, Liu T. The impact of urbanization on spatial-temporal variation in vegetation phenology: a case study of the Yangtze River Delta. China Remote Sens. 2024;16(5):914. doi:10.3390/rs16050914.
26. Zhong J, Liu J, Jiao L, Geiß C, Droin A, Taubenböck H. Unveiling the spatio-temporal patterns of vegetation growth influenced by diverse urban intensity gradients. Environ Impact Assess Rev. 2025;112(1):107810. doi:10.1016/j.eiar.2025.107810.
27. Miao L, He Y, Kattel GR, Shang Y, Wang Q, Zhang X. Double effect of urbanization on vegetation growth in China's 35 cities during 2000–2020. Remote Sens. 2022;14(14):3312. doi:10.3390/rs14143312.
28. Zhang Y, Ye A. Quantitatively distinguishing the impact of climate change and human activities on vegetation in mainland China with the improved residual method. GISci Remote Sens. 2021;58(2):235–60. doi:10.1080/15481603.2021.1872244.
29. Shi S, Smith L. Decoupling growth from degradation: a CS-ARDL and MMQR panel analysis of ecological footprints and sustainable economic growth. Front Environ Sci. 2025;13:1604011. doi:10.3389/fenvs.2025.1604011.

30. Xu R, Chen G. Does China's outward direct investment decrease carbon intensity in ASEAN countries? Evidence from CS-ARDL model analysis. Int J Clim Change Strateg Manag. 2025;17(1):529–44. doi:10.1108/ijccsm-07-2024-0120.
31. Kripfganz S, Schneider DC. Ardl: estimating autoregressive distributed lag and equilibrium correction models. Stata J Promot Commun Stat Stata. 2023;23(4):983–1019. doi:10.1177/1536867x231212434.
32. Chandra Voumik L, Sultana T. Impact of urbanization, industrialization, electrification and renewable energy on the environment in BRICS: fresh evidence from novel CS-ARDL model. Heliyon. 2022;8(11):e11457. doi:10.1016/j.heliyon.2022.e11457.
33. Zhao S, Liu S, Zhou D. Prevalent vegetation growth enhancement in urban environment. Proc Natl Acad Sci U S A. 2016;113(22):6313–8. doi:10.1073/pnas.1602312113.
34. Sadiq M, Chau KY, Ha NTT, Phan TTH, Ngo TQ, Huy PQ. The impact of green finance, eco-innovation, renewable energy and carbon taxes on CO_2 emissions in BRICS countries: evidence from CS ARDL estimation. Geosci Front. 2024;15(4):101689. doi:10.1016/j.gsf.2023.101689.
35. Chudik A, Pesaran MH. Common correlated effects estimation of heterogeneous dynamic panel data models with weakly exogenous regressors. J Econom. 2015;188(2):393–420. doi:10.1016/j.jeconom.2015.03.007.
36. Li X, Gong P, Zhou Y, Wang J, Bai Y, Chen B, et al. Mapping global urban boundaries from the global artificial impervious area (GAIA) data. Environ Res Lett. 2020;15(9):094044. doi:10.1088/1748-9326/ab9be3.
37. Gong P, Li X, Wang J, Bai Y, Chen B, Hu T, et al. Annual maps of global artificial impervious area (GAIA) between 1985 and 2018. Remote Sens Environ. 2020;236:111510. doi:10.1016/j.rse.2019.111510.
38. Pesaran MH. Estimation and inference in large heterogeneous panels with a multifactor error structure. Econometrica. 2006;74(4):967–1012. doi:10.1111/j.1468-0262.2006.00692.x.
39. Shao H, Qu M, Zhang Y, Zhang W. Regional differences in the direct and indirect impacts of China's urbanization process on vegetation. Earth Space Sci. 2026;13(4):e2026EA005001. doi:10.1029/2026ea005001.